Progress In Electromagnetics Research Letters, Vol. 48, 109–115, 2014

Design of Novel Compact Tri-Band Bandpass Filter with Controllable Frequencies and High Selectivity

Qian Fei Su*

Abstract—This paper presents a compact tri-band bandpass filter (BPF) with high selectivity. The proposed filter utilizes novel stub-loaded quarter-wavelength resonators and conventional uniform quarter-wavelength resonators. The latter is embedded in the former, and they are separated by a feed line. Due to these quarter-wavelength resonators, the total size is greatly reduced. Moreover, the passband frequencies can be controlled individually. To enhance its selectivity, source-load coupling is employed. For demonstration, an experimental filter is implemented. High skirt selectivity and suppression levels are observed in the measured results. The circuit area of the filter is $0.17\lambda_g \times 0.19\lambda_g$, featuring compact size.

1. INTRODUCTION

With the development of wireless communication, the multi-band telecommunication systems have shown their strong potential since they can reduce the size and loss of the whole systems. Bandpass filters, which are used to reject the unwanted signals, have gained a lot of attention. Recently, designing of novel tri-band filters have become very popular.

A widely used method is to utilize tri-section stepped-impedance resonators (SIRs) [1–4]. By controlling the electrical length and impedance ratios, the first three resonant frequencies can be controlled. In [1], a planar tri-band filter is realized with SIRs. Unfortunately, it suffers from poor selectivity. To improve it, source-load coupling is introduced [2]. However, the center frequencies of the three bands are dependent, which makes the design procedures complex. The second popular method is to use stub-loaded resonators [5–12]. In [5], tri-band responses are realized by open stub-loaded resonators. By controlling the open stub, the resonant frequencies can be easily tuned, whereas the size is bulky. To reduce the total size, a short stub-loaded resonator is utilized to obtain tri-band performance [6]. However, these structures are limited by their controlling ranges. To extent the tuning range, stub-load resonators can be combined with SIRs, which can realize large frequency ratio and provide sufficient degree of freedom [8–11]. In [9], a high-selectivity tri-band filter is realized by utilizing open stub-loaded resonators. Besides open-ended resonators, the stub-loaded short-ended resonators are also utilized to design tri-band filter. However, this method also suffers from dependent frequencies. To solve this problem, multi-sets of resonators are used [13–[17]. In [13], three different sets of resonators operating at three different passbands are assembled to design tri-band filters. However, it occupies large area. To reduce the size, one set of resonators is embedded in the other set of resonators is proposed [14, 15]. Besides the above methods, stub-loaded resonator combined with embedded multi-sets of resonators also can be employed [16, 17]. In the above references, most of the utilized stub-loaded resonators are stub-loaded half-wavelength resonators. Moreover, the stubs are usually located at the middle of the main transmission lines. Few researches focus on stub-loaded quarter-wavelength resonators.

Received 1 July 2014, Accepted 21 August 2014, Scheduled 25 August 2014
* Corresponding author: Qian Fei Su (qianfeisu@163.com).
The author is with the TP-Link Technology Co. Ltd, Shenzhen 518000, China.

In this paper, we present a novel miniaturized tri-band bandpass filter with high selectivity. The filter is designed by utilizing two sets of quarter-wavelength resonators, and the frequencies of the three passbands can be controlled individually. Source-load coupling is utilized to generate transmission zeros at both edges of each passband. To verify the presented idea, an experimental filter is implemented. Good agreement between simulated and measured results validates the prediction.

2. STUB-LOADED QUARTER-WAVELENGTH RESONATOR

Figure 1 shows the structure of the proposed stub-loaded quarter-wavelength resonator. It consists of a main short-end transmission line with characteristic admittance Y_1 and electrical length $\theta_1 + \theta_3$, and an open-stub with characteristic admittance Y_2 and electrical length θ_2. The input admittance of the proposed resonator can be expressed as:

$$Y_{\text{in}} = Y_1 \frac{-jY_1 \cot\theta_3 + jY_2 \tan\theta_2 + jY_1 \tan\theta_1}{Y_1 + j(-jY_1 \cot\theta_3 + jY_2 \tan\theta_2)\tan\theta_1} \tag{1}$$

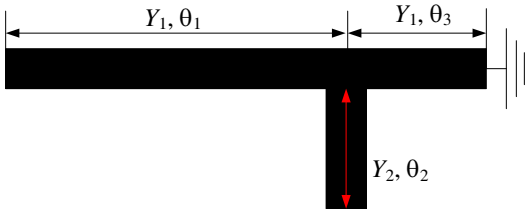

Figure 1. The proposed novel stub-loaded quarter-wavelength resonator.

The resonant frequencies can be obtained from $\text{Im}[Y_{in}] = 0$. To simplify the process, $Y_1 = Y_2$ is assumed. Thus, we can obtain

$$\tan\theta_1 + \tan\theta_2 = \cot\theta_3 \tag{2}$$

The first two roots of Equation (2) are set as f_1 and f_3. To analyze the resonant modes of the resonator, we define two electronic length ratios:

$$K_1 = \frac{\theta_3}{\theta_1 + \theta_3} \quad K_2 = \frac{\theta_2}{\theta_1 + \theta_3} \tag{3}$$

Combining Equations (2) and (3), the solutions of f_1 and f_3 can be obtained. Fig. 2 shows the frequency ratio of f_3/f_1 against K_1 and K_2. With different combinations of K_1 and K_2, the ratio can be changed from 1.5 to 3, which is suitable for designing dual-band applications with large frequency ratio.

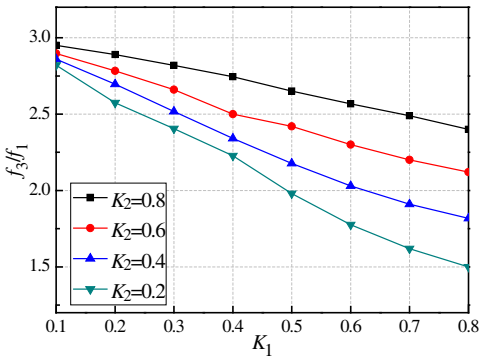

Figure 2. Frequency ratio against K_1 and K_2.

3. DESIGN OF TRI-BAND BANDPASS FILTER

The configuration of the proposed bandpass filter is shown in Fig. 3. It consists of two sets of resonators. One is the proposed novel stub-loaded quarter-wavelength resonator, and the other is uniform quarter-wavelength resonator. The latter is embedded in the former, resulting in compact size. The outer resonators work at first and third passbands, and the inner resonator operates at the second passband. No cross coupling exists between the inner and outer resonators. Thus, the inner and outer resonators can be controlled independently. The feed line is arranged between the two resonators to provide suitable coupling strength. Meanwhile, source-load coupling is utilized to generate transmission zeros to enhance the selectivity. The filter with 0.1-dB second-order Chebyshev response is designed with following specifications: the center frequencies (f_1, f_2 and f_3) of the three bands are 2.4, 3.9 and 5.4 GHz. The 3 dB-bandwidths are 14, 11 and 14%, respectively.

As stated, f_1 and f_3 are determined by the outer resonator, and the frequency ratio is 2.25. According to Fig. 2, K_1 and K_2 can be determined with 0.2 and 0.38. Thus, the value of $L_3/(L_1+L_2+L_8)$ equals 0.2, and $L_8/(L_1+L_2+L_8)$ equals 0.38. f_2 is determined by the inner quarter-wavelength resonator. Thus $L_4 + L_9 + L_{10}$ is quarter guide-wavelength at f_2. Fig. 4 shows the passband frequencies against L_3 and L_4. It can be observed that when L_3 is changed, the third passband is altered, while the first and second passbands are nearly fixed. When L_4 is changed, only the second passband changes while the other two passbands are fixed. Thus, the frequencies of the three passbands can be controlled

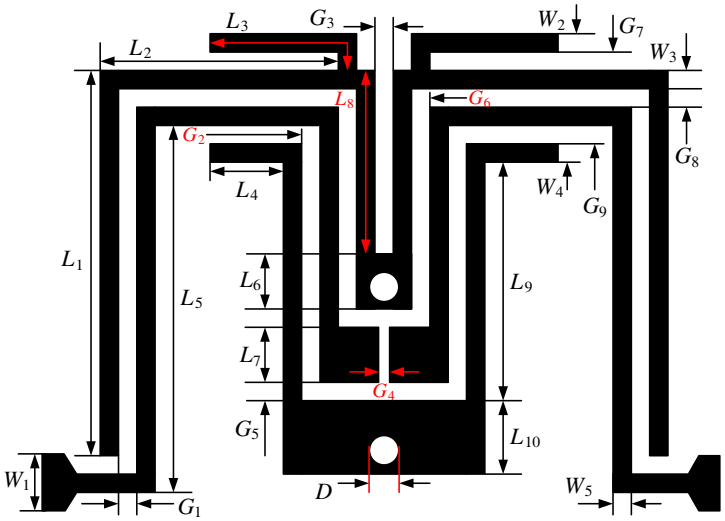

Figure 3. Structure of the proposed tri-band bandpass filter.

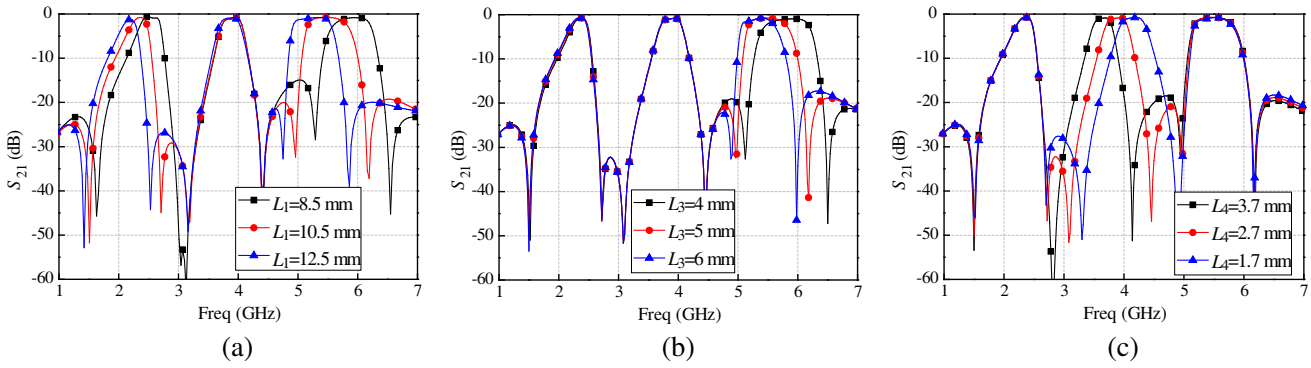

Figure 4. Passband frequencies against (a) L_1; (b) L_3; (c) L_4.

individually. We can first change the length of $L_1+L_2+L_8$ to obtain the first passband and then realize the third passband by changing L_3 and finally to obtain the second passband by tuning L_4 without affecting the other two bands.

The bandwidths of the tri-band filter depend on external quality factors (Q_es) and coupling coefficients (k_s). Q_e is determined by the coupling between the feed line and the resonators. Thus, for the first and third bands, Q_e is mainly determined by G_1, G_6 and G_8. For the second band, Q_e is mainly controlled by G_2 and G_9. Meanwhile, Q_e can be extracted from the simulation result based on full-wave simulator IE3D, and it can be calculated by [18]:

$$Q_e = \frac{f_0}{\Delta f_{\pm 90^o}} \tag{4}$$

where f_0 is the resonant frequency, and $\Delta f_{\pm 90^\circ}$ is the bandwidth over which the phase shifts $\pm 90^\circ$ with respect to the absolute phase at f_0. Fig. 5 illustrates Q_e against G_8, G_1 and G_2. Q_{e1}, Q_{e2} and Q_{e3} denote the external quality factors at first, second and third passbands, respectively. It can be observed that when G_8 becomes large, Q_{e1} becomes large, and Q_{e3} becomes small while Q_{e2} is fixed. When G_1 changes, only Q_{e3} changes while Q_{e1} and Q_{e2} are fixed. And G_2 only changes Q_{e2} as expected. Thus, Q_e at three bands can be controlled individually.

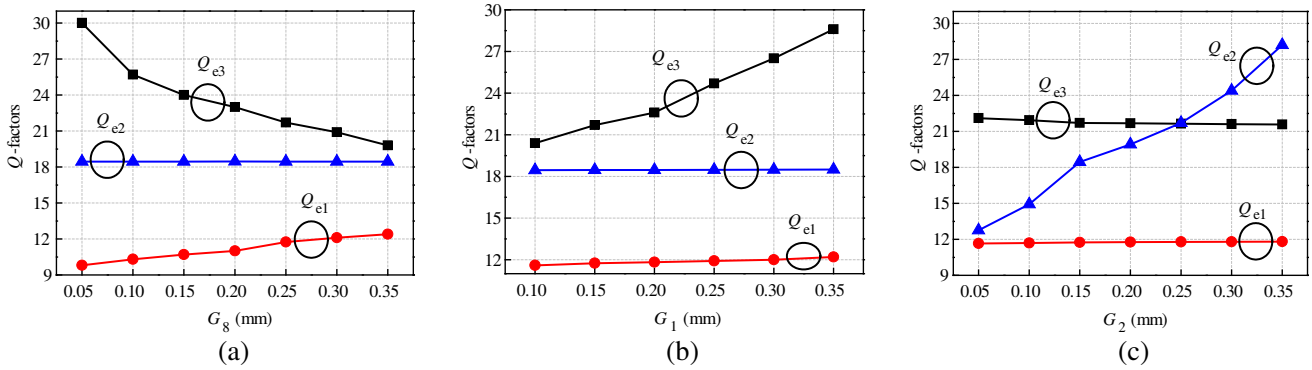

Figure 5. Q-factors against (a) G_8; (b) G_1; (c) G_2.

The coupling coefficient can be determined by the inner-coupling between the resonators, which can also be calculated as follows [18]:

$$k = \frac{f_{m2}^2 - f_{m1}^2}{f_{m2}^2 + f_{m1}^2} \tag{5}$$

where f_{m1} and f_{m2} are the higher and lower resonant frequencies, respectively. For the second band, k is mainly determined by L_{10}. Fig. 6(a) shows the extracted k against L_{10}. k_1, k_2 and k_3 denote the coupling coefficients at first, second and third passbands. It can be observed large L_{10} results in large k_2 and fixed k_1 and k_3. For the first and third bands, k is mainly controlled by G_3 and L_6. Fig. 6(b) illustrates k against G_3 and L_6. Different combinations can change k_1 from 0.1 to 0.19 and change k_3 from 0.07 to 0.16. With these figures, we can easily determine the initial values according to different specifications.

Since the stub is folded, the gap between the resonator and the stub may influence the performance of the filter. Fig. 7 shows the simulated results against G_7. It can be observed that when G_7 increases, the operating frequency of the third passband is slightly decreased and the coupling slightly enhanced. This may be due to the discontinuity which is brought by the folded stubs. The selectivity of the filter should also be taken into consideration. To enhance the selectivity, source-load coupling is utilized. The coupling strength is controlled by L_7 and G_4. Moreover, large L_7 and small G_4 make the transmission zeros close the passbands. Fig. 8 shows the simulated S_{21} against G_4. It can be observed that when G_4 is chosen as 0.6 mm, there are only four transmission zeros, while when G_4 becomes small, there are six transmission zeros, and the transmission zeros are closer to the passbands. Meanwhile, the performance of the passband is nearly fixed.

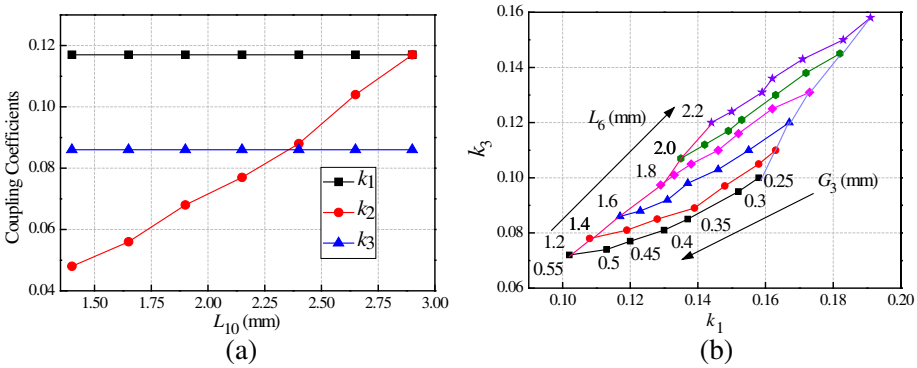

Figure 6. Coupling coefficients against (a) L_{10}, (b) G_3 and L_6.

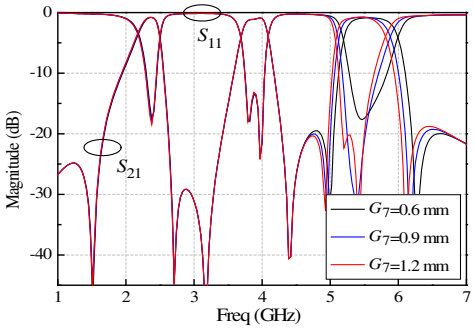

Figure 7. Simulated results against G_7.

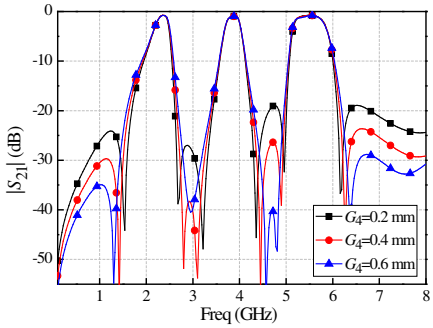

Figure 8. Simulated $|S_{21}|$ against G_4.

Thus, the design method can be summarized as follows: firstly, according to f_1 and f_3, we can determine K_1 and K_2. Referring K_1 and K_2, the lengths of $L_1 + L_2$, L_3 and L_8 can be determined. Then, according to f_2, the length of $L_4 + L_9 + L_{10}$ can be determined. After that, the bandwidth-related parameters should be determined. According to the bandwidths of the second passband, the coupling gaps G_2, G_9 and length L_{10} can be determined since they only affect the second passband. Then according to the bandwidths of the first and third passbands, the coupling gaps G_1, G_6, G_8 and lengths L_6, L_8 can be approximately determined. Till now, the operating frequency and bandwidths are obtained. Then L_7 and G_4 are used to realize high selectivity. Finally, fine tuning is used to obtain the whole performance.

4. FILTER IMPLEMENT

Based on the above analysis, a tri-band bandpass filter with high selectivity is designed and fabricated. The substrate has a relative dielectric constant of 3.38, thickness of 0.81 mm and loss tangent of 0.0027. The parameters are chosen as follows: $W_1 = 1.86\,\text{mm}$, $W_2 = W_3 = W_4 = 0.4\,\text{mm}$, $W_5 = 0.5\,\text{mm}$, $L_1 = 10.5\,\text{mm}$, $L_2 = 6.4\,\text{mm}$, $L_3 = 4.8\,\text{mm}$, $L_4 = 2.7\,\text{mm}$, $L_5 = 10.5\,\text{mm}$, $L_6 = 1.6\,\text{mm}$, $L_7 = 2.9\,\text{mm}$, $L_8 = 4.4\,\text{mm}$, $L_9 = 8\,\text{mm}$, $L_{10} = 1.9\,\text{mm}$, $G_1 = G_2 = 0.15\,\text{mm}$, $G_3 = 0.55\,\text{mm}$, $G_4 = 0.2\,\text{mm}$, $G_5 = 0.5\,\text{mm}$, $G_6 = 0.15\,\text{mm}$, $G_7 = 0.9\,\text{mm}$, $G_8 = G_9 = 0.25\,\text{mm}$, $D = 0.8\,\text{mm}$. The overall size of the fabricated filter is $12.9\,\text{mm} \times 14.8\,\text{mm}$ or $0.17\lambda_g \times 0.19\lambda_g$, where λ_g is the guide-wavelength of the lowest passband frequency. A photograph of the fabricated filter is shown in Fig. 9.

The simulation and measurement are accomplished by using IE3D and E5071C network analyzer, respectively. Fig. 10 compares the simulated and measured results. The passbands are centered at 2.4, 3.86 and 5.4 GHz, with 3 dB bandwidth of 13.5%, 10.9% and 13.2%. The minimum insertion loss is measured to be 1.4, 1.2 and 1.6 dB at the three passbands. The return loss is greater than 15 dB in all the passbands. There is a little difference between the simulated and measured results, which is due to the fabrication error. Six transmission zeros are generated at 1.44, 2.75, 3.1, 4.45, 4.92 and

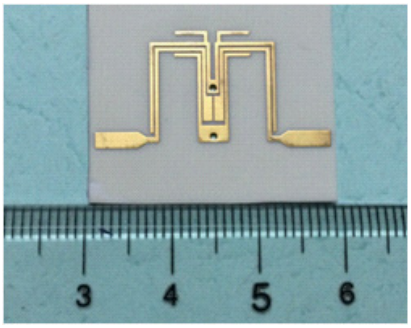

Figure 9. Photograph of the fabricated filter.

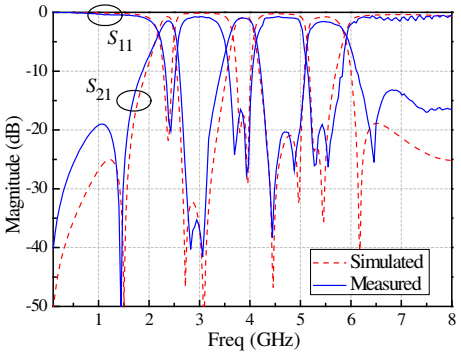

Figure 10. Simulated and measured results of the tri-band bandpass filter.

Table 1. Comparison with Prior Work FBW is the 3-dB bandwidth. FC denotes the frequency controllable, λ_g is the guide-wavelength of the lowest passband.

	Frequencies (GHz)	Insertion Loss (dB)	FBW(%)	FC	Transmission Zeros	Size ($\lambda_g \times \lambda_g$)
[3]	2.42/3.6/5.4	1/1.2/2.5	5.6/7.6/5.8	N	3	0.4×0.21
[9]	1.58/2.4/3.5	1.6/1.5/2.3	5.2/3.8/4.6	N	5	0.4×0.36
[11]	1.5/2.45/3.5	1.2/1/2.2	7.5/5.8/3.6	N	3	0.28×0.11
[12]	1.57/2.4/3.5	0.8/0.5/1.2	11.5/17.5/5.7	Y	4	0.25×0.1
[16]	2.45/3.5/5.2	1.2/1.5/1.6	9.6/13.1/7.9	Y	4	0.27×0.18
This work	2.4/3.86/5.4	1.4/1.2/1.6	13.5/10.9/13.2	Y	6	0.19×0.17

6.21 GHz. Due to these transmission zeros, high selectivity and high suppression level of adjacent bands are realized. Table 1 compares the proposed work with some prior designs which also focus on tri-band bandpass filters. It can be observed that the proposed work realizes a tri-band filter with controllable frequencies, high selectivity and compact size.

5. CONCLUSION

A tri-band bandpass filter utilizing novel stub-loaded and uniform quarter-wavelength resonators has been proposed. Due to these resonators, compact size is realized. And the passband frequencies can be individually controlled. The design methodology and experimental results have been presented. The bandpass filter has a compact size of $0.17\lambda_g \times 0.19\lambda_g$. Two transmission zeros are realized at both edges of each passband, resulting in high selectivity. The compact size and high selectivity make it attractive for wireless communication applications.

REFERENCES

1. Chu, Q.-X. and X.-M. Lin, "Advanced triple-band bandpass filter using tri-section SIR," *Electron. Lett.*, Vol. 44, No. 4, 295–296, 2008.
2. Hus, C. I. G., C. H. Lee, and Y. H. Hsieh, "Tri-band bandpass filter with sharp passband skirts designed using tri-section SIRs," *IEEE Microw. Wireless Compon. Lett*, Vol. 18, No. 1, 19–21, 2008.
3. Liu, B. and Y. Zhao, "Compact tri-band bandpass filter for WLAN and WiMAX using tri-section stepped-impedance resonators," *Progress In Electromagnetics Research Letters*, Vol. 45, 39–44, 2014.

4. Li, J., S. S. Huang, and J. Z. Zhao, "Design of a compact and high selectivity tri-band bandpass filter using asymmetric stepped-impedance resonators (SIRs)," *Progress In Electromagnetics Research Letters*, Vol. 44, 81–86, 2014.
5. Chen, F.-C., J.-M. Qiu, and Q.-X. Chu, "Design of compact tri-band bandpass filter using centrally loaded resonator," *Microwave Opt. Tech. Lett.*, Vol. 55, No. 11, 2695–2699, 2013.
6. Fan. W. X., Z. P. Li, and S. X. Gong, "Tri-band filter using combined E-type resonators," *Electron. Lett.*, Vol. 49, No. 1, 193–194, 2013.
7. Gao, L., X. Y. Zhang, B.-J. Hu, and Q. Xue, "Novel stub-loaded multi-mode resonators and their applications to various bandpass filters," *IEEE Trans. Microw. Theory Tech.*, Vol. 62, No. 5, 1162–1172, 2014.
8. Li, Z., T. Su, and C. Zhao, "A novel compact triple-passband design based on stepped impedance stub-loaded resonators," *Microw. Opt. Tech. Lett.*, Vol. 54, No. 9, 2106–2108, 2012.
9. Chen, W.-Y., M.-H. Weng, and S.-H. Chang, "A new tri-band bandpass filter based on stub-loaded step-impedance resonator," *IEEE Microw. Wireless Compon. Lett.*, Vol. 22, No. 4, 179–181, 2012.
10. Ghatak, R., M. Pal, P. Sarkar, A. K. Aditya, and D. R. Poddar, "Tri-band bandpass filters using modified tri-section stepped impedance resonator with improved selectivity and wide upper stopband," *IET Microw. Antennas Propag.*, Vol. 7, No. 15, 1187–1193, 2013.
11. Sun, S.-J., T. Su, K. Deng, B. Wu, and C.-H. Liang, "Shorted-ended stepped-impedance dual-resonance resonator and its application to bandpass filters," *IEEE Trans. Microw. Theory Tech.*, Vol. 61, No. 9, 3209–3215, 2013.
12. Chen, F. C., Q. X. Chu, and Z.-H. Tu, "Tri-band bandpass filter using stub loaded resonators," *Electron. Lett.*, Vol. 44, No. 12, 747–749, 2008.
13. Chen, F. C. and Q. X. Chu, "Design of compact tri-band bandpass filters using assembled resonators," *IEEE Trans. Microw. Theory Tech.*, Vol. 57, No. 1, 165–171, 2009.
14. Deng, H.-W., Y.-J. Zhao, X.-J. Zhou, Y. Fu, and Y.-Y. Liu, "Design of compact and high selectivity tri-band wideband microstrip BPF," *Microwave Opt. Technol. Lett.*, Vol. 55, No. 2, 258–261, 2013.
15. Peng, Y., L. Zhang, Y. Leng, and J. Guan, "A compact tri-band passband filter based on three embedded bending stub resonators," *Progress In Electromagnetics Research Letters*, Vol. 37, 189–197, 2013.
16. Xu. K., Y. Zhang, D. Li, Y. Fan, J. L.-W. Li, W. T. Joine, and Q. H. Liu, "Novel design of a compact triple-band bandpass filter using short stub-loaded SIRs and embedded SIRs structure," *Progress In Electromagnetics Research*, Vol. 142, 309–320, 2013.
17. Zhang, S. and L. Zhu, "Compact tri-band bandpass filter based on $\lambda/4$ resonators with U-folded coupled-line," *IEEE Microw. Wireless. Compon. Lett.*, Vol. 23, No. 5, 258–260, 2013.
18. Hong, J. S. and M. J. Lancaster, *Microwave Filter for RF/Microwave Application*, John Wiley & Sons, New York, 2001.